Comparing Aircraft Observations of Snowfall to Forecasts Using Single or Two Moment Bulk Water Microphysics Schemes

Andrew L. Molthan
Earth Science Office, Marshall Space Flight Center, Huntsville, AL

High resolution weather forecast models with explicit prediction of hydrometeor type, size distribution, and fall speed may be useful in the development of precipitation retrievals, by providing representative characteristics of frozen hydrometeors. Several single or double-moment microphysics schemes are currently available within the Weather Research and Forecasting (WRF) model, allowing for the prediction of up to three ice species. Each scheme incorporates different assumptions regarding the characteristics of their ice classes, particularly in terms of size distribution, density, and fall speed. In addition to the prediction of hydrometeor content, these schemes must accurately represent the vertical profile of water vapor to account for possible attenuation, along with the size distribution, density, and shape characteristics of ice crystals that are relevant to microwave scattering.

An evaluation of a particular scheme requires the availability of field campaign measurements. The Canadian CloudSat/CALIPSO Validation Project (C3VP) obtained measurements of ice crystal shapes, size distributions, fall speeds, and precipitation during several intensive observation periods. In this study, C3VP observations obtained during the 22 January 2007 synoptic-scale snowfall event are compared against WRF model output, based upon forecasts using four single-moment and two double-moment schemes available as of version 3.1. Schemes are compared against aircraft observations by examining differences in size distribution, density, and content. In addition to direct measurements from aircraft probes, simulated precipitation can also be converted to equivalent, remotely sensed characteristics through the use of the NASA Goddard Satellite Data Simulator Unit. Outputs from high resolution forecasts are compared against radar and satellite observations emphasizing differences in assumed crystal shape and size distribution characteristics.

Comparing Aircraft Observations of Snowfall to Forecasts Using Single or Two-Moment Bulk Water Microphysics Schemes

Andrew L. Molthan
NASA Short-term Prediction Research and Transition (SPoRT) Center, Marshall Space Flight Center, Huntsville, AL
andrew.molthan@nasa.gov
A11B-0037

Introduction

❖ High resolution forecast models use single or double-moment microphysics schemes to simulate the evolution and precipitation of various hydrometeors.
❖ Model output can be used to generate representative cloud and precipitation profiles for use within satellite simulators, assisting in the development of precipitation and cloud property retrievals.
❖ These schemes include various assumptions about particle size distribution, mass-diameter, and diameter-fall speed relationships, requiring evaluation.
❖ Here, field campaign data from the Canadian CloudSat/CALIPSO Validation Project (C3VP) is used to evaluate assumptions from single- and double-moment microphysics schemes available in the Weather Research and Forecasting (WRF) Model as of version 3.1.1.
❖ C3VP intensive observation periods included observations from dual-polarimetric radar, the CloudSat radar, aircraft, and surface instrumentation.
❖ Results here are presented from observations acquired during a widespread, synoptic-scale snowfall event on 22 January 2007 (Figure 1).

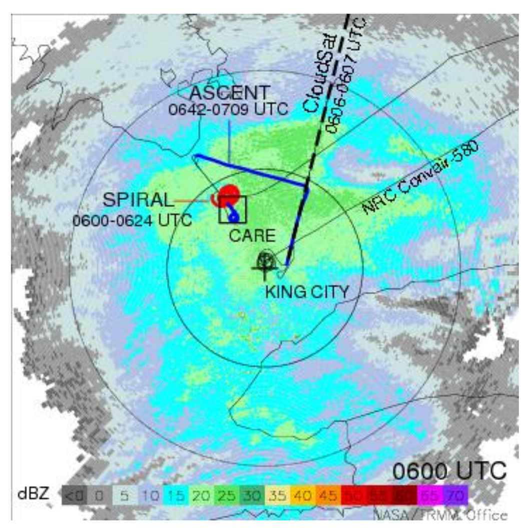

Figure 1. Observations available during the C3VP intensive observation period on 22 January 2007, overlaid upon horizontally polarized radar reflectivity at 0.8°, acquired from the dual-polarimetric, C-band radar at King City, Ontario.

Methodology

❖ The snowfall event was simulated with the WRF model, version 3.1.1, using six different single- or double-moment microphysics schemes. Forecasts use a triply nested grid configuration (9-3-1 km) with forcing provided by GFS analyses, and other parameterizations described within Molthan et al. 2010.
❖ Aircraft data were separated into two vertical profiles: a descending spiral near the radar site, and departure ascent. Measured particle sizes and quantities were used to estimate moments and size distribution shape characteristics to compare against scheme assumptions.
❖ The 0600 UTC model output period was selected because observed precipitation rates were nearly steady, the radar indicated wide coverage of moderate precipitation, and each forecast produced a reasonable depiction of precipitation intensity and coverage during this time period.
❖ WRF model vertical profiles were extracted within 50 km of the King City radar and averaged to compare mean model conditions against the aircraft spiral and aircraft ascent profile data.

Snow Characteristics in Selected Microphysics Schemes

Goddard	• Single-moment • Fixed distribution intercept • Fixed density spheres	Tao et al. 2003 Shi et al. 2010
WSM6	• Single-moment • Size distribution intercept a function of temperature • Fixed density spheres	Hong et al. 2005
Thompson	• Single-moment • Predicts snow content, then other moments as a function of snow mass and temperature. • Non-spherical mass-diameter relationship	Thompson et al. 2008
SBU-Lin	• Single-moment • Snow characteristics range from dry to graupel-like via diagnosed riming factor, Ri. • Distribution intercept is a function of temperature • Predicts mass-diameter, diameter-fall speed, and PSD characteristics based upon Ri	Lin et al. 2010 Lin and Colle 2010
WDM6	• Double moment rain category	Hong et al. 2010
Morrison	• Double moment in all species • Fixed density spheres	Morrison et al. 2005

Hydrometeor Profiles

❖ Ice water content measured onboard the aircraft via a counterflow virtual impactor (CVI, Twohy et al. 1997). Although liquid water measurements were also available, no appreciable liquid water content was reported (Figure 2).
❖ Conditional mean profiles of hydrometeor content were produced from WRF model profiles within 50 km of the King City radar.
❖ All schemes generally reproduce the aircraft vertical profiles of ice water content, although some place greater emphasis on small cloud ice crystals. None of the forecasts produced significant amounts of graupel.
❖ The dominance of the snow category is supported by C3VP and radar observations of ice crystals and aggregates throughout the vertical column.

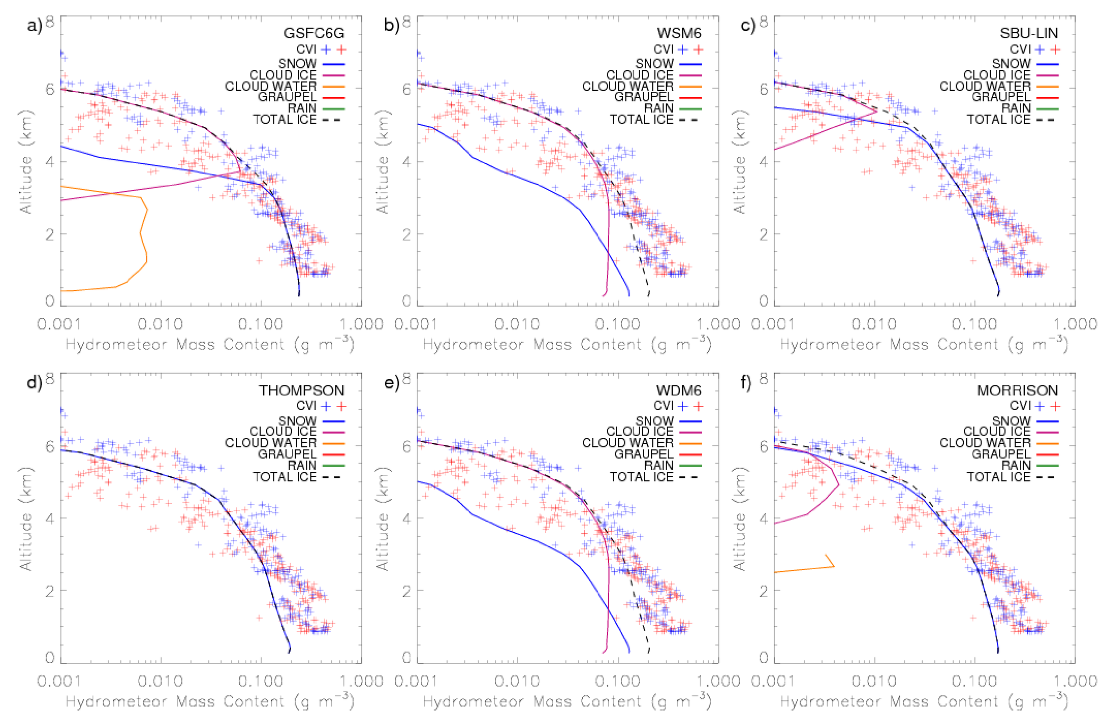

Figure 2. Conditional mean profiles of hydrometeor content acquired from WRF simulated profiles within 50 km of the King City radar.

Water Vapor Profiles

❖ Mean profiles of water vapor differ substantially among the forecasts and are shown in terms of relative humidity in Figure 3.
❖ Differences are likely attributable to the saturation adjustment process within each scheme, deposition or sublimation terms.
❖ The majority of aircraft observations reported an environment saturated (supersaturated) with respect to water (ice).
❖ The Goddard scheme performs well until temperatures cool to -15°C, then is affected by the saturation adjustment scheme selected for this simulation.
❖ The WSM6/WDM6 forecasts produced an environment unsaturated with respect to water throughout the vertical column, but with slight ice supersaturation.
❖ The Thompson and Morrison schemes follow the general trend in observations, while the SBU-Lin forecast smoothly decreases saturation with respect to water at altitudes above 2 km.

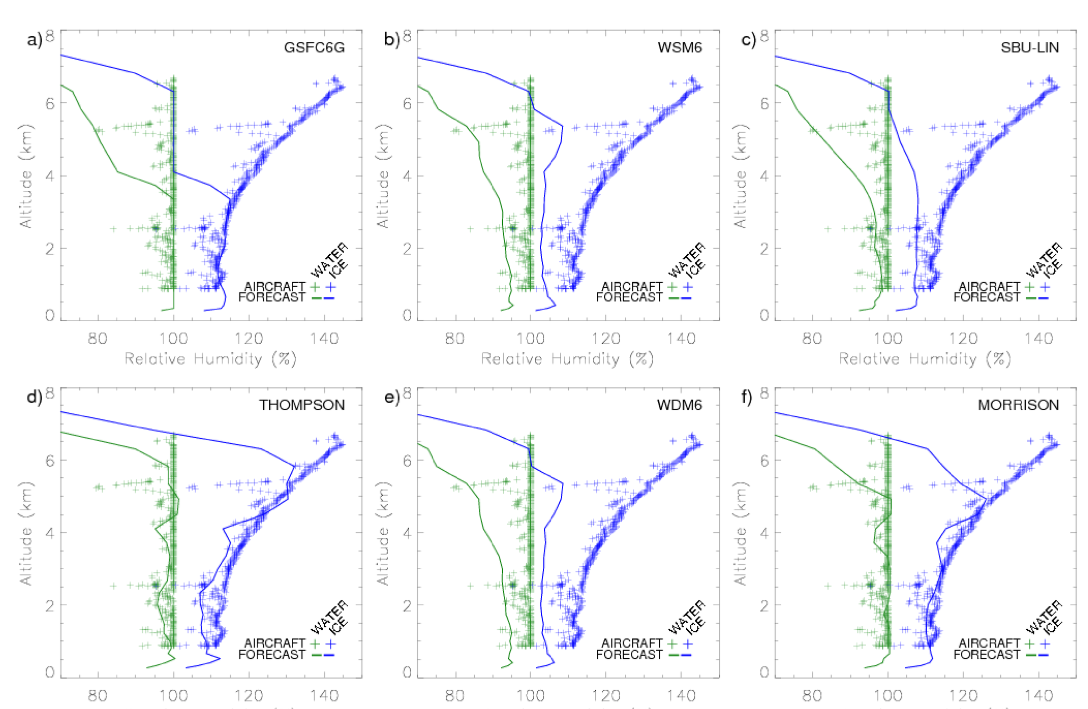

Figure 3. Conditional mean profiles of relative humidity with respect to water and ice, acquired from WRF profiles within 50 km of the King City radar.

Size Distribution Parameters

❖ Aircraft measurements included imaging probes with crystal imagery used to construct particle size distributions (PSDs) binned by maximum diameter.
❖ Although the Thompson scheme uses a very specific PSD, remaining schemes use a generalized gamma distribution (1), with dispersion parameter μ set to zero, resulting in an exponential size distribution.

$$N(D)=N_{os}D^{\mu}e^{-\lambda_s D} \quad (1)$$

❖ Exponential size distributions were fit to each five second aircraft PSD with parameters retained if the resulting best-fit distribution was well-fit to observations ($R^2 \geq 0.8$).
❖ Size distribution parameters were obtained from model output data based upon their assumed PSD characteristics or parameterizations. Resulting variables were converted to mean profiles acquired within 50 km of the King City radar (Figure 4).

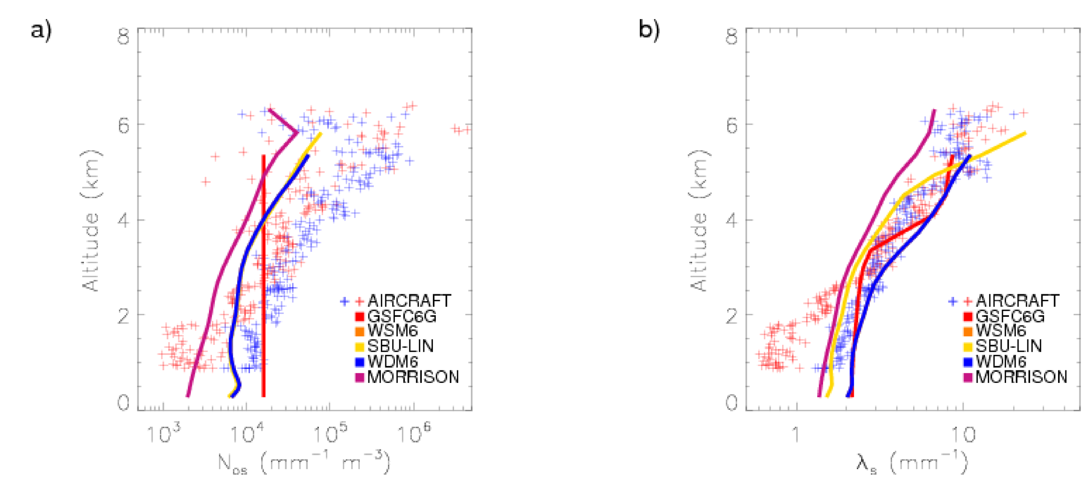

Figure 4. a) Aircraft estimates of the size distribution intercept parameter in (1), along with model mean profiles from applicable forecast schemes. b) As in a) but for the distribution slope parameter.

Comparing Moments of Size Distributions

❖ Particle size distributions were also compared by examining their moments. This is particularly valuable for the Thompson scheme, which predicts the second moment of the PSD and infers remaining moments as a function of temperature.
❖ Relationships in the Thompson scheme are based upon aircraft measurements of ice crystals and temperature-dependent functions between moments, as described by Field et al. 2007.
❖The n^{th} moment, or M_n, can be calculated as:

$$M_n = N_{os}\Gamma(1+\mu+n) \,/\, \lambda^{(1+\mu+n)} \quad (2)$$

❖ Resulting comparisons between aircraft PSDs and model profiles are shown for select moments in Figure 5. Model profiles for the Thompson scheme are based upon temperature-dependent relationships used within the forecast.
❖ Double moment representation in the Morrison scheme provides a better depiction of aggregation effects. Other vertical trends in aircraft observations are best represented by schemes that provide flexibility in PSD characteristics.

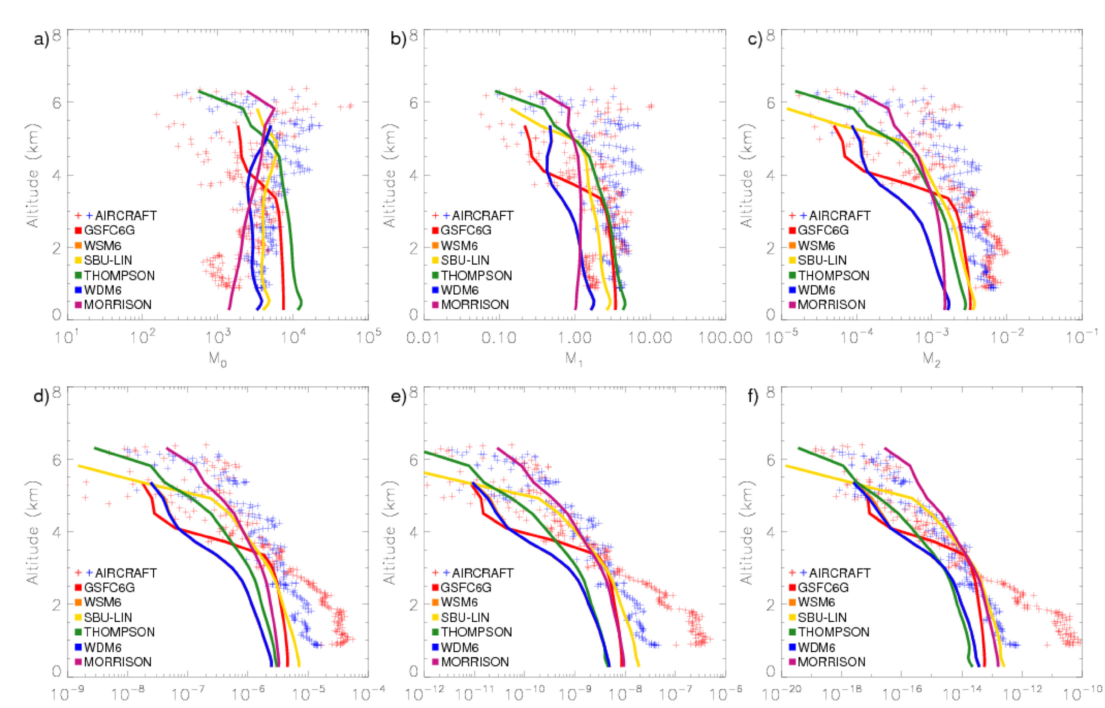

Figure 5. Comparison of various PSD moments estimated from aircraft data versus mean profiles of moments acquired from model simulated profiles.

Terminal Velocities

❖ Terminal velocity and diameter relationships combine with PSDs and simulated mass content to determine precipitation and flux rates.
❖ Surface observations of fall speeds were provided by the Hydrometeor Velocity and Shape Detector (HVSD, Barthazy et al. 2004) at the CARE site, northwest of the King City radar.
❖ HVSD data were binned by particle maximum dimension, then combined in a joint histogram by size and fall speed increments of 5 cm s^{-1}.
❖ Observations and fits limited to particles 1 mm or greater.
❖ A power-law fit was acquired for C3VP observations and compared to similar functional forms used within each scheme (Figure 6.)

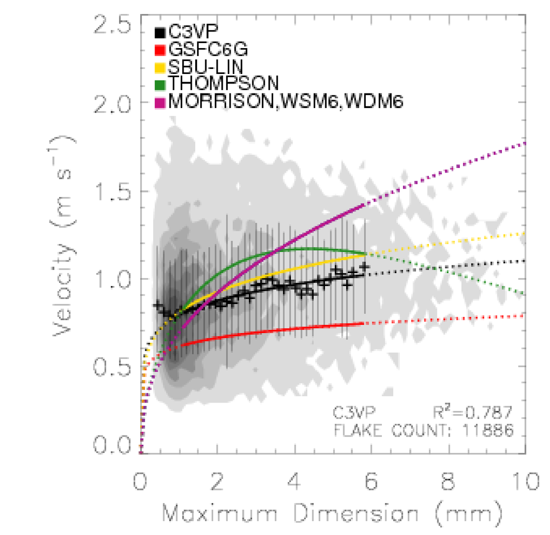

Figure 6. Joint histogram of particle maximum dimension and fall speed from the HVSD, along with best-fit C3VP relationship and other equations used to describe fall speeds within each forecast scheme.

Implications for Simulating Remote Sensors

❖ Satellite simulators have been developed, generating proxies for remote sensors from high resolution forecast model output (Matsui et al. 2009).
❖ Model simulated profiles of hydrometeor content and remotely sensed quantities may facilitate the development of satellite-based retrievals.
❖ One challenge in this process is the representation of scattering by complex ice crystal shapes. Molthan et al. 2010 simulated CloudSat 94 GHz radar reflectivity, from various non-spherical shapes and demonstrated a better fit than Mie spheres.
❖ To avoid mismatched assumptions, the mass-diameter relationship within the forecast model should match the characteristics of simulated crystals, such as those described by Liu (2008) and aggregates of Ishimoto (2008).
❖ Mass-diameter relationships and common model assumptions are compared in Figure 7a. The asymmetry parameters of two Liu 2008 crystal types are compared in Figure 7b for a variety of frequencies within the Liu 2010 database.

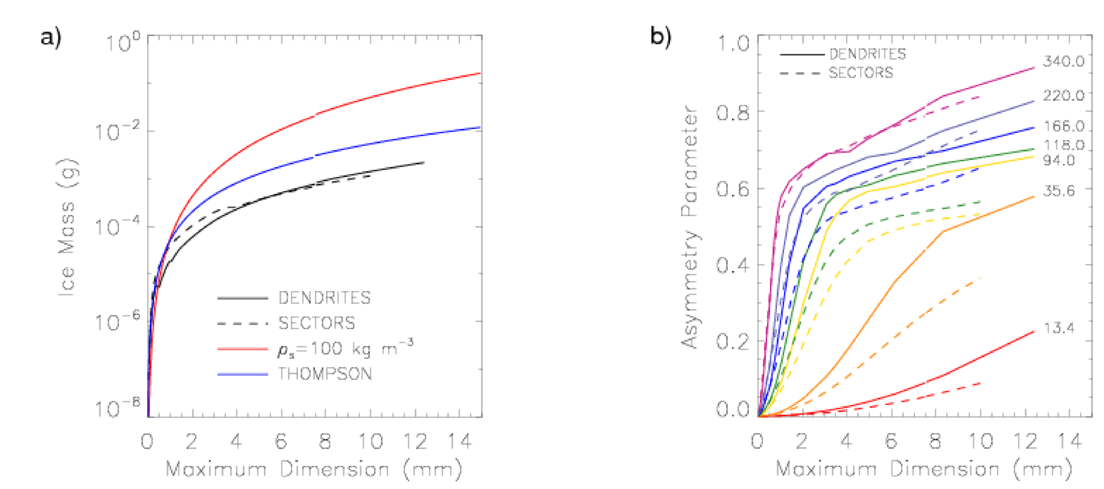

Figure 7. a) Mass-diameter relationships from selected forecast model assumptions versus Liu 2008 dendrites and sector plates. b) Comparison of the asymmetry parameter for Liu 2008 crystal habits at a variety of frequencies.

Future Work

❖ Use aircraft PSDs and other C3VP data sets to evaluate the simulation of satellite products for this event.
❖ Select a single- or double-moment scheme and incorporate flexibility in mass-diameter relationships to provide for a match to crystal database entries.
❖ Verify that the WRF simulated microphysics, PSDs, and crystal database entries produce a reasonable depiction of remotely sensed quantities and attempt to use model profiles toward the retrieval of cloud properties.

Acknowledgements and References

❖ The author would like to thank David Hudak, Steve Nesbitt, and Walt Petersen for their assistance in utilizing and interpreting C3VP-related data.
❖ An experimental version of the SBU-Lin scheme and installation steps were provided by Yanluan Lin and Brian Colle for use in this study.
❖ A complete list of references is available upon request.